Applied Mathematical Modelling 137 (2025) 115716

Contents lists available at ScienceDirect

Applied Mathematical Modelling

journal homepage: www.elsevier.com/locate/apm

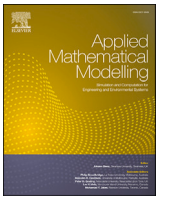

Solution for time-dependent resilience in the presence of gradual deterioration of performance

Cao Wang

School of Civil and Environmental Engineering, University of Technology Sydney, Ultimo, NSW 2007, Australia

ARTICLE INFO

Keywords:
Time-dependent resilience
Performance deterioration
Closed-form solution
Resilience-based design

ABSTRACT

In this paper, a closed-form method is developed for the evaluation of time-dependent resilience (so named as it is a function of the service time of interest) of an aging object (e.g., a structure or system). These structures and systems often suffer from the deterioration of performances in a harsh service environment, causing the decline of serviceability. They are thus expected to be sufficiently resilient during their service lives, i.e., to have the ability to withstand disruptions to their performances. The proposed method takes into account the uncertainty associated with the performance deterioration process, the availability of resources that support the performance recovery, and the impact of a changing environment. The accuracy and improved efficiency of the proposed method are demonstrated through three examples. It is also shown through sensitivity analysis that the impact of a changing environment, and the availability of recovery-supporting resources play an essential role in the time-dependent resilience. The proposed resilience method can also be used to efficiently guide the design of new structures that meet predefined resilience goals.

1. Introduction

Structures and infrastructure systems play an essential role in supporting modern societies' functionalities, but suffer from gradual deterioration of performance in their service lives due to environmental attacks such as corrosion [1]. Due to the uncertainties arising from the environmental factors and the properties of an object (structure or system), the serviceability cannot be evaluated in a deterministic manner. With this regard, resilience assessment has gained significant research interests recently, which probabilistically measures the ability of an object to withstand, recover from, and adapt to disruptions [2]. The focus of this paper is on the resilience of aging objects within a reference period of interest (e.g., the life cycle), which is referred to as "time-dependent resilience" [3] as it is dependent on the considered time duration. The evaluation of time-dependent resilience can be used to determine whether the life-cycle performance is satisfactory by comparing the resilience with a target level [3].

In [4], the life-cycle resilience of a deteriorating structure is measured by the accumulative performance loss to hazardous events. A renewal-reward process was used to model the occurrence of hazards. However, this resilience model is not applicable when the functionality deterioration is caused by continuous environmental factors (e.g., corrosion) but not a discrete hazard process. Iannacone et al. [5] proposed a formula to investigate the effects of infrastructure deterioration on the time-varying ability to recover after disruptive events. In [3], an explicit measure for the time-dependent resilience of repairable structures is developed by considering the impacts of structural performance deterioration and nonstationary external loads. However, these works have studied the resilience

E-mail address: cao.wang@uts.edu.au.

https://doi.org/10.1016/j.apm.2024.115716
Received 27 January 2024; Received in revised form 13 September 2024; Accepted 16 September 2024

Available online 23 September 2024

problem in the presence of discrete hazardous events, modeled by a Poisson stochastic process. There are many cases where the performance deterioration of an aging object is dominated by detrimental effects such as aggressive chemical attacks and other physical damage mechanisms [6–9]. When the performance of an object degrades to a predefined threshold, interventions (e.g., repair, or replacement) must be carried out to restore the deteriorated performance [10,11]. However, the resilience evaluation in the presence of gradually deteriorating performance has been limitedly addressed in previous studies. In [12], a simulation-based approach was proposed to evaluate the resilience of coastal building foundations considering soil strength deterioration due to water intrusion. The impacts of performance deterioration and climate change on resilience were investigated. However, it is computationally more costly to employ the Monte Carlo simulation in resilience assessment compared with closed form formulas. Further, explicit solutions may offer insights into the resilience problem which otherwise may be difficult to achieve through simulation-based methods.

The research question considered in this paper is: Can we evaluate the time-dependent resilience of an object (e.g., an individual structure, or a system) with a closed-form solution, considering the gradual deterioration of performance function? The establishment of such a method will be beneficial for asset owners/policy makers to efficiently and conveniently evaluate the structural and infrastructure resilience (e.g., without technical requirements on the skills for conducting Monte Carlo simulation). The resilience assessment can be further used to guide resilience-based design, life-cycle management and maintenance optimization [13–16]. For example, Ref. [13] summarized the role of resilience in risk-based asset management plans. In [15], a load and resistance factor design-like method was developed to guide the resilience-based design of individual structures. In [16], the selection of optimal retrofit strategy was studied that minimizes the life-cycle cost and simultaneously satisfies the resilience requirement of infrastructure.

The novelty of this paper is as follows,

1. A closed-form solution is proposed to evaluate the time-dependent resilience of an object (e.g., an individual structure, or a system) considering the gradual deterioration of performance over time.
2. The proposed method can incorporate the impact of a changing environment, where the deterioration rate of performance may be accelerated.
3. The proposed resilience method can be used to efficiently guide the design of new structures in the presence of a predefined resilience goal.

Three examples are presented in this paper to demonstrate the applicability of the proposed method. It is shown via sensitivity analysis that, in the presence of limited resources to recover the deteriorated performance, the resilience would be overestimated if considering an unchanged environment.

2. Closed-form resilience model with infinite resources

In this section, the resilience (see Definition 1) of a gradually-deteriorating object (e.g., a structure or system) over a reference period of $[0, t_l]$ will be derived.

Definition 1. The time-dependent resilience over the reference period of $[0, t_l]$, denoted by $\mathrm{Res}(t_l)$, is defined as follows [17],

$$\mathrm{Res}(t_l) = \mathbb{E}\left\{\exp\left[\frac{1}{t_l}\int_0^{t_l} \ln Q(t)dt\right]\right\} \tag{1}$$

in which $\mathbb{E}(\,)$ denotes the mean value of the variable in the brackets, and $Q(t)$ is the performance of an object at time t, taking a value between 0 and 1. It is in some cases more convenient to use the term "nonresilience", which equals 1 minus the resilience in Eq. (1).

In the presence of environmental attacks, the performance of the object, $Q(t)$, degrades gradually from 1 (i.e., full performance) at the initial time (where t is time), as shown in Fig. 1. Upon $Q(t)$ reaching a predefined threshold α (where $0 < \alpha < 1$), interventions (e.g., maintenance measures) are to be conducted to restore the performance. Let Δ be the time duration for $Q(t)$ degrading from 1 to α. We will proceed based on the following assumption.

Assumption 1. Taking into account the uncertainty associated with Δ, the Gamma distribution type is assumed for Δ with a shape parameter of a and a scale parameter of b. This is motivated by the fact that Gamma distribution has a support of $(0, \infty)$, and can describe different shapes of distribution (it may reduce to Erlang, exponential, chi-squared, Schulz–Zimm and normal distribution types with properly selected scale and shape parameters).

Let δ be the recovery time (i.e., the duration that $Q(t)$ is restored from α to 1), which is modeled as a deterministic value due to its negligible uncertainty compared with that of Δ. Based on Assumption 1, the probability density function (PDF) of Δ takes a form of the following,

$$f_\Delta(x) = \frac{(x/b)^{a-1}}{b\Gamma(a)}\exp\left(-\frac{x}{b}\right) \tag{2}$$

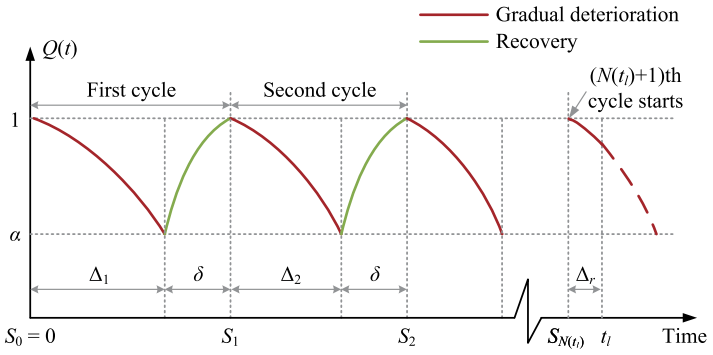

Fig. 1. Time-dependent performance of an aging object over $[0, t_l]$.

in which Γ is the Gamma function. The gradual deterioration process of $Q(t)$ is modeled as follows,

$$Q(t) = 1 - K \cdot t^{\eta} \tag{3}$$

where K is a random variable reflecting the deterioration rate, and $\eta > 0$ is a deterministic parameter that defines the shape of the deterioration process. For example, if $\eta = 1$, then the performance degrades linearly. Other values of η (e.g., 0.5, or 2) result in varying deterioration rates within $[0, \Delta]$. According to Eq. (3), it follows that $\alpha = 1 - K \cdot \Delta^{\eta}$, with which K is a generalized inverse Gamma variable (see the definition in, e.g., [18]). For a specific case where Δ follows an exponential distribution, then K follows an Extreme Type II distribution. Similar to Eq. (3), the recovery process is also featured by a shape parameter θ that allows for the flexibility of modeling different recovery shapes, i.e., for $t \in [\Delta, \Delta + \delta]$, it follows that, $Q(t) = \alpha + \frac{1-\alpha}{\delta^{\theta}}(t - \Delta)^{\theta}$.

The process from initial state to fully restored state is called a "cycle" (the duration of a cycle is $\Delta + \delta$). For the ith cycle within $[0, t_l]$ $(i = 1, 2, \ldots)$, a subscript of "i" is introduced for Δ. Note that the recovery process of $Q(t)$ is supported by the availability of resources (e.g., labour, and finance). This section focuses on the resilience problem with "infinite resources", that is, there is no limit on the number of recovery processes. The impact of resource availability on resilience will be later addressed in Sect. 3.

Denote $\widetilde{\Delta}_m = \sum_{i=1}^{m} \Delta_i, m = 1, 2, \ldots$, and define

$$S_0 = 0, \quad S_m = \sum_{i=1}^{m} (\Delta_i + \delta) = \widetilde{\Delta}_m + m\delta, \quad m = 1, 2, \ldots \tag{4}$$

Let $N(t_l)$ be the number of cycles (see Fig. 1 for illustration) within the time interval $[0, t_l]$, that is, $N(t_l) = \max\{m : S_m \le t_l\}$. In Eq. (4), each Δ_i follows a Gamma distribution with a shape parameter of a_i and a scale parameter of b for $i = 1, 2, \ldots m$. Here, the shape parameter of each Δ_i is not necessarily identical, which allows for the flexibility of modeling a nonstationary deterioration sequence in a changing environment. Since δ is a deterministic value, an upper bound for $N(t_l)$ exists, i.e., $N(t_l) \le m_u := \lfloor \frac{t_l}{\delta} \rfloor$, where $\lfloor x \rfloor$ denotes the maximum integer that does not exceed x. For a nonnegative integer $m = 0, 1, 2, \ldots$, it follows that,

$$\mathbb{P}(N(t_l) \le m) = \mathbb{P}\left(S_{m+1} > t_l\right) = 1 - \mathbb{P}\left(\widetilde{\Delta}_{m+1} \le t_l - (m+1)\delta\right) \tag{5}$$

where $\mathbb{P}(\,)$ denotes the probability of the event in the brackets. Note that $\widetilde{\Delta}_m$ follows a Gamma distribution according to Eq. (4), with a shape parameter of $\sum_{i=1}^{m} a_i$ and a scale parameter of b for $m = 1, 2, \ldots$. The cumulative distribution function (CDF) and PDF of $\widetilde{\Delta}_m$ are denoted by $F_{\widetilde{\Delta}_m}(x)$ and $f_{\widetilde{\Delta}_m}(x)$, respectively, for $m = 1, 2, \ldots$.

Define an auxiliary variable Δ_0, whose CDF is as follows, $F_{\widetilde{\Delta}_0}(x) = \mathbf{1}(x > 0)$, where $\mathbf{1}(\,)$ is an indicator function, returning a value of 1 if the statement in the brackets is true and 0 otherwise. With this, the PDF of Δ_0 is $f_{\widetilde{\Delta}_0}(x) = \mathfrak{d}(x)$, in which $\mathfrak{d}$ is the Dirac delta function, satisfying $\int_{-\infty}^{\infty} \mathfrak{d}(x)dx = 1$.

Note that $F_{\widetilde{\Delta}_m}(x) = 0$ if $x < 0$ for $m = 0, 1, 2, \ldots$. With this, Eq. (5) becomes, $\mathbb{P}(N(t_l) \le m) = 1 - F_{\widetilde{\Delta}_{m+1}}\left(t_l - (m+1)\delta\right)$, $m = 0, 1, 2, \ldots$. This further gives the probability mass function (PMF) of $N(t_l)$ as follows,

$$\mathbb{P}(N(t_l) = m) = F_{\widetilde{\Delta}_m}\left(t_l - m\delta\right) - F_{\widetilde{\Delta}_{m+1}}\left(t_l - (m+1)\delta\right), \quad m = 0, 1, 2, \ldots m_u \tag{6}$$

Define the forward recurrence time, denoted by Δ_r, as: $\Delta_r = t_l - S_{N(t_l)}$. Note that

$$\begin{aligned} \mathbb{P}(N(t_l) = m \cap \Delta_r \le x) &= \mathbb{P}\left(S_m < t_l \cap S_{m+1} > t_l \cap S_m > t_l - x\right) \\ &= \mathbb{P}\left(\max\left(t_l - x - m\delta, t_l - \Delta_{m+1} - (m+1)\delta\right) < \widetilde{\Delta}_m < t_l - m\delta\right) \end{aligned} \tag{7}$$

Since $\widetilde{\Delta}_m$ is independent of Δ_{m+1}, it follows that,

$$\begin{aligned}\mathbb{P}(N(t_l)=m\cap\Delta_r\le x)&=\int_0^{\infty}\left[F_{\widetilde{\Delta}_m}\left(t_l-m\delta\right)-F_{\widetilde{\Delta}_m}\left(\max\left(t_l-x-m\delta,t_l-y-(m+1)\delta\right)\right)\right]\cdot f_{\Delta_{m+1}}(y)\,dy\\&=F_{\widetilde{\Delta}_m}\left(t_l-m\delta\right)-\int_0^{\infty}F_{\widetilde{\Delta}_m}\left(\max\left(t_l-x-m\delta,t_l-y-(m+1)\delta\right)\right)\cdot f_{\Delta_{m+1}}(y)\,dy\\&=F_{\widetilde{\Delta}_m}\left(t_l-m\delta\right)-F_{\widetilde{\Delta}_m}\left(t_l-x-m\delta\right)\cdot\int_{x-\delta}^{\infty}f_{\Delta_{m+1}}(y)\,dy\\&\quad-\int_0^{x-\delta}F_{\widetilde{\Delta}_m}\left(t_l-y-(m+1)\delta\right)\cdot f_{\Delta_{m+1}}(y)\,dy\end{aligned}\tag{8}$$

Combining Eqs. (6) and (8), one can obtain the conditional CDF of Δ_r on $N(t_l)=m$, denoted by $F_{\Delta_r|N(t_l)=m}(x)$, by noting that,

$$F_{\Delta_r|N(t_l)=m}(x)=\mathbb{P}(\Delta_r\le x|N(t_l)=m)=\frac{\mathbb{P}(N(t_l)=m\cap\Delta_r\le x)}{\mathbb{P}(N(t_l)=m)}\tag{9}$$

Further, the conditional PDF of Δ_r on $N(t_l)=m$ is evaluated as follows,

$$f_{\Delta_r|N(t_l)=m}(x)=\frac{g(x,m)}{\mathbb{P}(N(t_l)=m)}\tag{10}$$

in which $g(x,m)$ takes a form of the following for $m=0,1,2,\dots m_u$ according to the Leibniz integral rule,

$$\begin{aligned}g(x,m)&=f_{\widetilde{\Delta}_m}\left(t_l-x-m\delta\right)\cdot\left[1-F_{\Delta_{m+1}}(x-\delta)\right]+F_{\widetilde{\Delta}_m}\left(t_l-x-m\delta\right)\cdot f_{\Delta_{m+1}}(x-\delta)\\&\quad-F_{\widetilde{\Delta}_m}\left(t_l-(x-\delta)-(m+1)\delta\right)\cdot f_{\Delta_{m+1}}(x-\delta)\\&=f_{\widetilde{\Delta}_m}\left(t_l-x-m\delta\right)\cdot\left[1-F_{\Delta_{m+1}}(x-\delta)\right]\end{aligned}\tag{11}$$

From Eq. (10), it is observed that,

$$\int_0^{\infty}g(x,m)dx=\mathbb{P}(N(t_l)=m)\tag{12}$$

Remark 1. An alternative approach to derive $g(x,m)$ in Eq. (10) is as follows. Note that,

$$\begin{aligned}\lim_{dx\to0}g(x,m)\cdot dx&=\mathbb{P}(x<\Delta_r\le x+dx\cap N(t_l)=m)\\&=\mathbb{P}(t_l-(x+dt)\le S_m<t_l-x\cap\Delta_{m+1}+\delta>x)\\&=\mathbb{P}(t_l-(x+dt)-m\delta\le\widetilde{\Delta}_m<t_l-x-m\delta\cap\Delta_{m+1}>x-\delta)\\&=f_{\widetilde{\Delta}_m}\left(t_l-x-m\delta\right)\cdot\left[1-F_{\Delta_{m+1}}(x-\delta)\right]\cdot dt\end{aligned}\tag{13}$$

which yields the same result as in Eq. (11).

The remaining of this section is aimed to derive the explicit solution for $\mathrm{Res}(t_l)$.

First, for the time interval of $[0,\Delta_1]$, according to Eq. (3), one has,

$$\int_0^{\Delta_1}\ln Q(t)dt=\int_0^{\Delta_1}\ln\left(1-\frac{1-\alpha}{\Delta_1^{\eta}}t^{\eta}\right)dt=\psi_1(\eta,\alpha)\cdot\Delta_1\tag{14}$$

in which $\psi_1(\eta,\alpha)=\ln\alpha-(\alpha-1)\cdot\Phi_L\left(1-\alpha,1,1+\frac{1}{\eta}\right)$, where Φ_L is the Lerch transcendent, defined as $\Phi_L(x,y,z)=\sum_{i=0}^{\infty}\frac{x^i}{(i+z)^y}$.

If some representative values of η are considered, the expression of $\psi_1(\eta,\alpha)$ can be simplified. For example, with $\eta=0.5$, 1 or 2 (corresponding to square-root, linear or parabolic deterioration shape, respectively), it follows that,

$$\psi_1(\eta,\alpha)=\begin{cases}\dfrac{2(\alpha-2)\alpha\ln\alpha-\alpha^2+4\alpha-3}{2(\alpha-1)^2}, & \eta=0.5\\ \dfrac{\alpha\ln\alpha}{\alpha-1}-1, & \eta=1\\ \dfrac{2\tanh^{-1}\left(\sqrt{1-\alpha}\right)}{\sqrt{1-\alpha}}+\ln\alpha-2, & \eta=2\end{cases} \tag{15}$$

Next, for the time interval of $[\Delta_1,\Delta_1+\delta]$, it follows that,

$$\int_{\Delta_1}^{\Delta_1+\delta}\ln Q(t)dt=\int_{\Delta_1}^{\Delta_1+\delta}\ln\left(\alpha+\frac{1-\alpha}{\delta^\theta}(t-\Delta_1)^\theta\right)dt=\int_0^{\delta}\ln\left(\alpha+\frac{1-\alpha}{\delta^\theta}\tau^\theta\right)d\tau=\psi_2(\theta,\alpha)\cdot\delta \tag{16}$$

where $\psi_2(\theta,\alpha)=\frac{\alpha-1}{\alpha}\Phi_L\left(\frac{\alpha-1}{\alpha},1,1+\frac{1}{\theta}\right)$.

With some specific values of θ, one has,

$$\psi_2(\theta,\alpha)=\begin{cases}\dfrac{2\alpha^2\ln\alpha+\alpha(4-3\alpha)-1}{2(\alpha-1)^2}, & \theta=0.5\\ \dfrac{\alpha\ln\alpha}{\alpha-1}-1, & \theta=1\\ \dfrac{2\alpha\tan^{-1}\left(\sqrt{\frac{1}{\alpha}-1}\right)}{\sqrt{\alpha(1-\alpha)}}-2, & \theta=2\end{cases} \tag{17}$$

Based on Eqs. (14) and (16), the resilience in Eq. (1) is rewritten as follows,

$$\mathrm{Res}(t_l)=\mathbb{E}\left\{\exp\left[\frac{1}{t_l}\left(\psi_1\sum_{i=1}^{N(t_l)}\Delta_i+\psi_2 N(t_l)\delta+H(\Delta_r)\right)\right]\right\} \tag{18}$$

where $H(\Delta_r)=\int_{t_l-\Delta_r}^{t_l}\ln Q(t)dt$. Note that $\sum_{i=1}^{N(t_l)}\Delta_i+N(t_l)\delta+\Delta_r=t_l$, with which

$$\mathrm{Res}(t_l)=\mathbb{E}\left\{\exp\left[\frac{1}{t_l}\left(N(t_l)\delta(\psi_2-\psi_1)+H(\Delta_r)-\psi_1\Delta_r+\psi_1 t_l\right)\right]\right\} \tag{19}$$

Based on the law of total probability, one has,

$$\begin{aligned}\mathrm{Res}(t_l)&=\sum_{m=0}^{m_u}\mathbb{P}(N(t_l)=m)\cdot\mathbb{E}\left\{\exp\left[\frac{1}{t_l}\left(N(t_l)\delta(\psi_2-\psi_1)+H(\Delta_r)-\psi_1\Delta_r+\psi_1 t_l\right)\right]\middle| N(t_l)=m\right\}\\&=\sum_{m=0}^{m_u}\mathbb{P}(N(t_l)=m)\cdot\int_0^{t_l-m\delta}\mathbb{E}\left\{\exp\left[\frac{m\delta}{t_l}(\psi_2-\psi_1)+\frac{H(x)-\psi_1 x}{t_l}+\psi_1\right]\right\}\cdot f_{\Delta_r|N(t_l)=m}(x)dx\\&=\sum_{m=0}^{m_u}\int_0^{t_l-m\delta}\exp\left[\frac{m\delta}{t_l}(\psi_2-\psi_1)-\frac{\psi_1 x}{t_l}+\psi_1\right]\cdot\mathbb{E}\left\{\exp\left[\frac{H(x)}{t_l}\right]\right\}\cdot g(x,m)dx\end{aligned} \tag{20}$$

where the item $\mathbb{E}\left\{\exp\left[\frac{H(x)}{t_l}\right]\right\}$, as will be derived in the following, has been conditional on $\Delta_r=x$. With this regard, let Δ'_{m+1} be such a Δ_{m+1} that satisfies $\Delta'_{m+1}+\delta\geq x$, i.e., the PDF of Δ'_{m+1} is the same as that of Δ_{m+1} except its lower tail being truncated at $x-\delta$. With this, the PDF of Δ'_{m+1} is expressed as follows,

$$f_{\Delta'_{m+1}}(y)=\begin{cases}0, & \text{if } y<x-\delta\\ \dfrac{f_{\Delta_{m+1}}(y)}{1-F_{\Delta_{m+1}}(x-\delta)}, & \text{otherwise}\end{cases} \tag{21}$$

To derive $\mathbb{E}\left\{\exp\left[\frac{H(x)}{t_l}\right]\right\}$, the following two cases need to be considered, as shown in Fig. 2: at time t_l, the performance is either in the gradual deterioration process (Case 1) or in the recovery process (Case 2).

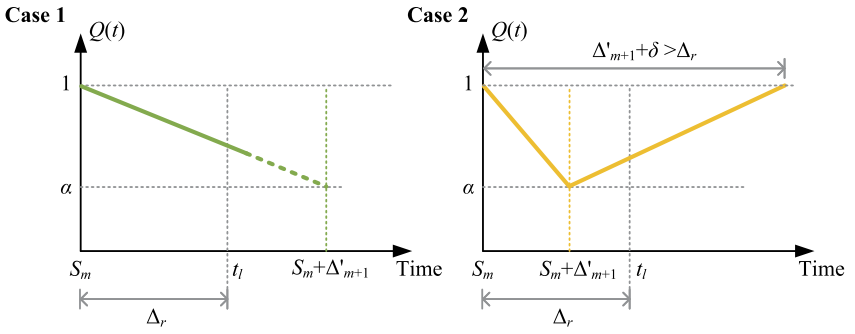

Fig. 2. Illustration of performance function at time t_l.

Combining the two scenarios in Fig. 2, it follows that,

$$\begin{aligned}\mathbb{E}\left\{\exp\left[\frac{H(x)}{t_l}\right]\right\} &= \int_x^{\infty}\exp\left(\frac{1}{t_l}\int_0^x \ln\left(1-\frac{1-\alpha}{y^{\eta}}t^{\eta}\right)dt\right)\cdot f_{\Delta'_{m+1}}(y)dy \\ &\quad+\int_{x-\delta}^{x}\exp\left(\frac{1}{t_l}\int_0^y \ln\left(1-\frac{1-\alpha}{y^{\eta}}t^{\eta}\right)dt\right)\cdot\exp\left(\frac{1}{t_l}\int_0^{x-y}\ln\left(\alpha+\frac{1-\alpha}{\delta^{\theta}}t^{\theta}\right)dt\right)\cdot f_{\Delta'_{m+1}}(y)dy \\ &= \int_x^{\infty}\exp\left(\frac{y}{t_l}\cdot\psi_3\left(\frac{x}{y},\alpha,\eta\right)\right)\cdot f_{\Delta'_{m+1}}(y)dy+\int_{x-\delta}^{x}\exp\left(\frac{y}{t_l}\cdot\psi_1(\alpha,\eta)+\frac{x-y}{t_l}\psi_4\left(\frac{x-y}{\delta},\alpha,\theta\right)\right)\cdot f_{\Delta'_{m+1}}(y)dy\end{aligned} \tag{22}$$

where

$$\psi_3(\rho,\eta,\alpha)=\begin{cases}\dfrac{2((\alpha-1)^2\rho-1)\ln\left(1+(\alpha-1)\sqrt{\rho}\right)+(\alpha-1)\left(2\sqrt{\rho}-(\alpha-1)\rho\right)}{2(\alpha-1)^2}, & \eta=0.5\\ \left(\dfrac{1}{\alpha-1}+\rho\right)\ln(1+\rho(\alpha-1))-\rho, & \eta=1\\ \dfrac{2\tanh^{-1}\left(\rho\sqrt{1-\alpha}\right)}{\sqrt{1-\alpha}}+\rho\left[\ln\left(1+\rho^2(\alpha-1)\right)-2\right], & \eta=2\end{cases} \tag{23}$$

and

$$\psi_4(\rho,\theta,\alpha)=\begin{cases}\dfrac{\frac{2\alpha^2\ln\alpha}{\rho}+(1-\alpha)\left(\alpha-1+\frac{2\alpha}{\sqrt{\rho}}\right)+2\left((\alpha-1)^2-\frac{\alpha^2}{\rho}\right)\ln\left(\alpha+\sqrt{\rho}-\alpha\sqrt{\rho}\right)}{2(\alpha-1)^2}, & \theta=0.5\\ \dfrac{\alpha\ln\left(1+\frac{1-\alpha}{\alpha}\rho\right)}{\rho(1-\alpha)}+\ln(\alpha+\rho(1-\alpha))-1, & \theta=1\\ \dfrac{2\alpha\tan^{-1}\left(\rho\sqrt{\frac{1}{\alpha}-1}\right)}{\rho\sqrt{\alpha(1-\alpha)}}+\ln\left(\rho^2+\alpha(1-\rho^2)\right)-2, & \theta=2\end{cases} \tag{24}$$

Denote

$$J_1(x,y,m)=\exp\left[\frac{m\delta}{t_l}(\psi_2-\psi_1)-\frac{\psi_1 x}{t_l}+\psi_1+\frac{y}{t_l}\cdot\psi_3\left(\frac{x}{y},\eta,\alpha\right)\right]\cdot f_{\Delta_{m+1}}(y)\cdot f_{\widetilde{\Delta}_m}\left(t_l-x-m\delta\right) \tag{25}$$

and

$$J_2(x,y,m)=\exp\left[\frac{m\delta}{t_l}(\psi_2-\psi_1)+\psi_1+\frac{x-y}{t_l}\left(\psi_4\left(\frac{x-y}{\delta},\theta,\alpha\right)-\psi_1\right)\right]\cdot f_{\Delta_{m+1}}(y)\cdot f_{\widetilde{\Delta}_m}\left(t_l-x-m\delta\right) \tag{26}$$

Combining Eq. (20) and (22), one has,

$$\mathrm{Res}(t_l)=\sum_{m=0}^{m_u}\left[\int_0^{t_l-m\delta}\int_x^{\infty}J_1(x,y,m)dydx+\int_0^{t_l-m\delta}\int_{x-\delta}^{x}J_2(x,y,m)dydx\right] \tag{27}$$

Eq. (27) presents the proposed closed-form solution for the time-dependent resilience in Eq. (1), by fully taking into account the uncertainties associated with the performance function over $[0,t_l]$. The accuracy and improved efficiency (compared with simulation-based method) will be later addressed in Sect. 4.

3. Closed-form resilience model with limited resources

Recall that in Eq. (27), the resilience model has been derived without considering the limit on the maximum number of recovery processes. There are many cases in engineering practice that, due to the budget/resource constraint, the deteriorated performance, upon reaching the threshold α, can be recovered for at most κ times, where κ is a nonnegative integer. This is the motivation for a revised form of Eq. (27) by taking into account the impact of κ on resilience. In particular, such an impact dominates when $S_\kappa \le t_l$, or equivalently, $N(t_l)\ge\kappa$.

Based on the definition of time-dependent resilience in Eq. (1), using the law of total probability, it follows that,

$$\begin{aligned}\mathrm{Res}(t_l,\kappa)=&\underbrace{\mathbb{E}\left\{\exp\left[\frac{1}{t_l}\int_0^{t_l}\ln Q(t)dt\right]\middle|N(t_l)\le\kappa-1\right\}\cdot\mathbb{P}(N(t_l)\le\kappa-1)}_{\text{part 1}}\\&+\underbrace{\mathbb{E}\left\{\exp\left[\frac{1}{t_l}\int_0^{t_l}\ln Q(t)dt\right]\middle|N(t_l)\ge\kappa\right\}\cdot\mathbb{P}(N(t_l)\ge\kappa)}_{\text{part 2}}\end{aligned} \tag{28}$$

in which the resilience is rewritten as $\mathrm{Res}(t_l,\kappa)$ because it is also a function of κ.

With Eq. (27), "part 1" of Eq. (28) is evaluated as follows,

$$\begin{aligned}&\mathbb{E}\left\{\exp\left[\frac{1}{t_l}\int_0^{t_l}\ln Q(t)dt\right]\middle|N(t_l)\le\kappa-1\right\}\cdot\mathbb{P}(N(t_l)\le\kappa-1)\\&=\sum_{m=0}^{\min(m_u,\kappa-1)}\left[\int_0^{t_l-m\delta}\int_x^{\infty}J_1(x,y,m)dydx+\int_0^{t_l-m\delta}\int_{x-\delta}^{x}J_2(x,y,m)dydx\right]\end{aligned} \tag{29}$$

The second part of Eq. (28) is associated with the case of $S_\kappa < t_l$, as will be discussed next. Define $\Delta_{r,\kappa}=t_l-S_\kappa$. Note that,

$$\begin{aligned}\mathbb{P}\left(N(t_l)\ge\kappa\bigcap\Delta_{r,\kappa}\le x\right)&=\mathbb{P}\left(S_\kappa\le t_l\bigcap t_l-S_\kappa\le x\right)\\&=\mathbb{P}(t_l-x\le\widetilde{\Delta}_\kappa+\kappa\delta\le t_l)\\&=F_{\widetilde{\Delta}_\kappa}(t_l-\kappa\delta)-F_{\widetilde{\Delta}_\kappa}(t_l-\kappa\delta-x)\end{aligned} \tag{30}$$

with which

$$\mathbb{P}\left(\Delta_{r,\kappa}\le x|N(t_l)\ge\kappa\right)=\frac{F_{\widetilde{\Delta}_\kappa}(t_l-\kappa\delta)-F_{\widetilde{\Delta}_\kappa}(t_l-\kappa\delta-x)}{\mathbb{P}\left(N(t_l)\ge\kappa\right)} \tag{31}$$

This yields the conditional CDF of $\Delta_{r,\kappa}$ on $N(t_l)\ge\kappa$, and further the conditional PDF, denoted by $f_{\Delta_{r,\kappa}|N(t_l)\ge\kappa}(x)$, as follows,

$$f_{\Delta_{r,\kappa}|N(t_l)\ge\kappa}(x)=\frac{f_{\widetilde{\Delta}_\kappa}(t_l-\kappa\delta-x)}{\mathbb{P}\left(N(t_l)\ge\kappa\right)},\quad 0\le x\le t_l-\kappa\delta \tag{32}$$

Denote $\Delta_{0,i}=\frac{\Delta_i}{(1-\alpha)^{1/\eta}},\quad i=1,2,\ldots$. Within the time interval $[S_\kappa,t_l]$, the two quantities $\Delta_{0,\kappa+1}$ and $\Delta_{r,\kappa}$ are compared to determine the performance scenario at time t_l, as illustrated in Fig. 3. Conditional on $\Delta_{0,\kappa+1}=x$, if $\Delta_{r,\kappa}>x$ (see Case 1 in Fig. 3), then the performance function $Q(t)$ degrades to zero before time t_l, with which $\int_{S_\kappa}^{t_l}\ln Q(t)dt=0$. Otherwise (i.e., $\Delta_{r,\kappa}\le x$, see Case 2 in Fig. 3), it follows that,

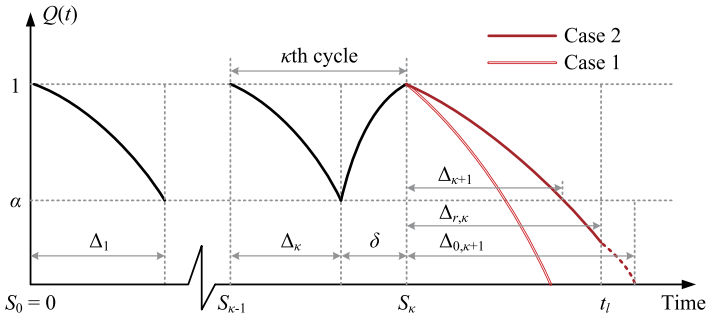

Fig. 3. Illustration of time-dependent resilience affected by κ.

$$\int_{S_\kappa}^{t_l} \ln Q(t)dt = \int_{S_\kappa}^{t_l} \ln\left(1-\frac{(t-S_\kappa)^\eta}{x^\eta}\right)dt = \int_0^{\Delta_{r,k}} \ln\left(1-\frac{t^\eta}{x^\eta}\right)dt = \psi_5\left(\frac{\Delta_{r,\kappa}}{x},\eta\right)\cdot\Delta_{r,\kappa} \tag{33}$$

where

$$\psi_5(\rho,\eta) = \rho^\eta \Phi_L\left(\rho^\eta, 1, 1+\frac{1}{\eta}\right) + \ln(1-\rho^\eta), \quad 0<\rho<1 \tag{34}$$

For some specific values of η, $\psi_5(\rho,\eta)$ is simplified as follows,

$$\psi_5(\rho,\eta) = \begin{cases} \left(1-\frac{1}{\rho}\right)\ln\left(1-\sqrt{\rho}\right) - \sqrt{\frac{1}{\rho}} - \frac{1}{2}, & \eta = 0.5 \\ \left(1-\frac{1}{\rho}\right)\ln(1-\rho) - 1, & \eta = 1 \\ \frac{2}{\rho}\tanh^{-1}(\rho) - 2 + \ln(1-\rho^2), & \eta = 2 \end{cases} \tag{35}$$

Note that the probability distribution of $\Delta_{\kappa+1}$ is independent of the condition of $N(t_l)\geq\kappa$. This is because, $\Delta_{\kappa+1}$ is independent of S_k by definition, and that $\mathbb{P}\left(N(t_l)\geq\kappa\right) = \mathbb{P}\left(S_\kappa \leq t_l\right)$. Thus, "part 2" of Eq. (28) is evaluated as follows,

$$\begin{aligned} &\mathbb{E}\left\{\exp\left[\frac{1}{t_l}\int_0^{t_l}\ln Q(t)dt\right]\middle| N(t_l)\geq\kappa\right\}\cdot\mathbb{P}\left(N(t_l)\geq\kappa\right) \\ &= \int_0^\infty \mathbb{E}\left\{\exp\left[\frac{1}{t_l}\int_0^{t_l}\ln Q(t)dt\right]\middle| N(t_l)\geq\kappa\cap\Delta_{0,\kappa+1}=x\right\} f_{\Delta_{0,\kappa+1}}(x)dx\cdot\mathbb{P}\left(N(t_l)\geq\kappa\right) \\ &= \int_0^\infty \int_0^{\min(x,t_l-\kappa\delta)} \exp\left[\frac{1}{t_l}\left(\psi_1(t_l-y-\kappa\delta)+\psi_2\kappa\delta+y\psi_5\left(\frac{y}{x},\eta\right)\right)\right]\cdot f_{\widetilde{\Delta}_\kappa}(t_l-\kappa\delta-y)\cdot f_{\Delta_{0,\kappa+1}}(x)dydx \end{aligned} \tag{36}$$

Denote

$$J_3(x,y) = \exp\left[\frac{1}{t_l}\left(\psi_1(t_l-y-\kappa\delta)+\psi_2\kappa\delta+y\psi_5\left(\frac{y}{x},\eta\right)\right)\right] f_{\widetilde{\Delta}_\kappa}(t_l-\kappa\delta-y) f_{\Delta_{0,\kappa+1}}(x) \tag{37}$$

With this, the resilience in Eq. (28) is rewritten as follows,

$$\mathrm{Res}(t_l,\kappa) = \sum_{m=0}^{\min(m_u,\kappa-1)}\left[\int_0^{t_l-m\delta}\int_x^\infty J_1(x,y,m)dydx + \int_0^{t_l-m\delta}\int_{x-\delta}^{x} J_2(x,y,m)dydx\right] + \int_0^\infty\int_0^{\min(x,t_l-\kappa\delta)} J_3(x,y)dydx \tag{38}$$

Eq. (38) is the proposed resilience method in the presence of limited resources that support the recovery of performance for at most κ times. The applicability of Eq. (38) will be demonstrated in the next section. Note that in Eq. (38), if $\kappa\to\infty$, then $\int_0^\infty\int_0^{\min(x,t_l-\kappa\delta)} J_3(x,y)dydx \to 0$, with which Eq. (38) reduces to Eq. (27).

Remark 2. In Eq. (38), if $\kappa = 0$, then

$$\sum_{m=0}^{\min(m_u,\kappa-1)} \left[\int_0^{t_l-m\delta} \int_x^{\infty} J_1(x,y,m)dydx + \int_0^{t_l-m\delta} \int_{x-\delta}^{x} J_2(x,y,m)dydx \right] = 0 \tag{39}$$

with which

$$\mathrm{Res}(t_l,\kappa) = \int_0^{\infty} \int_0^{\min(x,t_l)} J_{3,\kappa=0}(x,y)dydx \tag{40}$$

where $J_{3,\kappa=0}(x,y)$ is a specific form of $J_3(x,y)$ in Eq. (37) with $\kappa = 0$, i.e.,

$$J_{3,\kappa=0}(x,y) = \exp\left[\frac{1}{t_l}\left(\psi_1(t_l-y) + y\psi_5\left(\frac{y}{x},\eta\right)\right)\right] f_{\widetilde{\Delta}_0}(t_l-y) f_{\Delta_{0,1}}(x) \tag{41}$$

This further gives the resilience with $\kappa = 0$ as follows,

$$\mathrm{Res}(t_l,0) = \int_{t_l}^{\infty} \exp\left[\psi_5\left(\frac{t_l}{x},\eta\right)\right] f_{\Delta_{0,1}}(x)dx \tag{42}$$

In the context of "reliability", if the limit state is defined as $\Delta_{0,1} \geq t_l$, then the time-dependent reliability over $[0,t_l]$, denoted by $\mathrm{Rel}(t_l)$, is evaluated as follows,

$$\mathrm{Rel}(t_l) = \mathbb{P}(\Delta_{0,1} \geq t_l) = \int_{t_l}^{\infty} f_{\Delta_{0,1}}(x)dx \tag{43}$$

The similarity between Eqs. (42) and (43) suggests that, if not considering the recovery process of $Q(t)$, then the two quantities – reliability and resilience – can be evaluated in a unified framework. This can be explained by noting that, the reliability assessment focuses on the survival-state limit state, i.e., $Q(t) \in \{0,1\}$, which corresponds to the case of $\eta \to \infty$. Note also that, in Eq. (34), $\lim_{\eta\to\infty} \psi_5(\rho,\eta) = 0$. With this, based on the definition of reliability in Eq. (43), it follows that,

$$\mathrm{Rel}(t_l) = \lim_{\eta\to\infty} \underbrace{\mathrm{Res}(t_l,0)}_{\text{Eq. (42)}} \tag{44}$$

The proposed resilience models in Eqs. (27) and (38) have been derived based on an explicit form of the performance function $Q(t)$. For an individual structure, one may set the deterioration of performance to be in parallel with the time-variation of structural resistance (with this regard, one can refer to previous studies [19,20] for discussions on the probabilistic models of structural resistance deterioration). For a system consisting of interacting components (structures), the time-variation of system performance is dependent on the holistic behavior of the components, which may require a network analysis [21] to determine the deterioration process of system performance. For the case where only scattered data of the system performance at discrete time instants are available (e.g., due to the computational burdens of network analysis for a large-scale system), one can find an expression for $Q(t)$ based on Eq. (3) through least-squares fitting, with a focus on determining the deterioration shape and rate parameters.

4. Examples

4.1. Numerical example

In this section, a numerical example is presented to demonstrate the applicability of the proposed resilience models in Eqs. (27) and (38). Consider the resilience of an aging structure for a service period of 50 years. Its performance degrades, from 1 initially, with time during its service life due to environmental attacks. Upon the performance reaching 0.7 times the initial state, repair measures are immediately conducted to restore the structural performance to the full state. The duration of each recovery process is $\delta = 1$ year. The time it takes for the performance function to degrade from initial time by 30% (i.e., Δ_1) is a Gamma variable, with a mean value of 10 years and a coefficient of variation (COV) of 0.2. However, taking into account the impact of a changing environment, for the ith cycle ($i = 1,2,\ldots$), the mean value of Δ_i equals $10\exp(-\psi\cdot(i-1))$ years with a constant scale parameter, where ψ is the deteriorating rate of the mean value (a time-invariant constant). For example, if $\psi = 0.1$, then the performance deterioration from 1 to 0.7 takes on average 9.05 years during the second cycle, and 8.19 years for the third cycle.

Fig. 4 examines the impact of κ (i.e., the maximum number of recovery processes) on time-dependent nonresilience for reference periods up to 50 years, assuming $\eta = \theta = 1$, and $\psi = 0.1$. The nonresilience increases with the duration of service period, which is characteristic of the accumulation of degraded performance over time. A larger value of κ leads to smaller nonresilience due to the greater amount of resources that support the recovery of performance. The impact of κ on resilience is enhanced with a longer

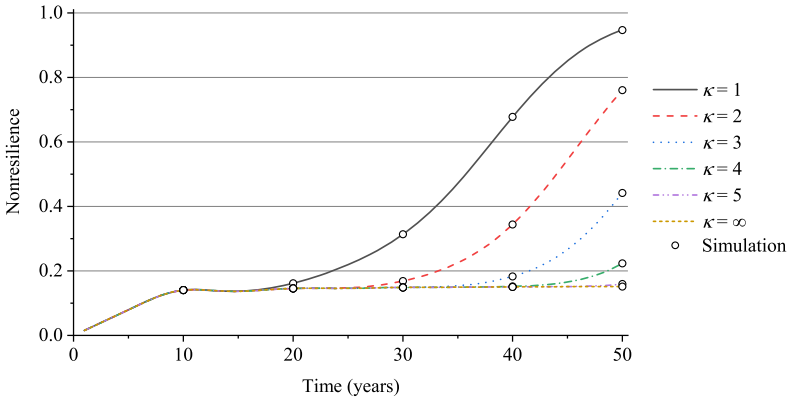

Fig. 4. Impact of κ on time-dependent nonresilience.

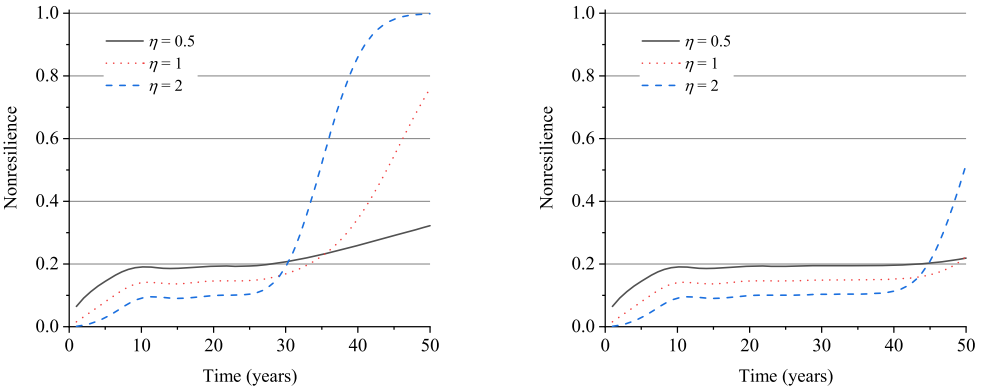

(a) $\kappa = 2$ (b) $\kappa = 4$

Fig. 5. Dependence of nonresilience on η (assuming $\theta = 1$).

reference period, where the number of recovery processes plays a dominating role. For instance, for reference periods up to 18 years, the difference between the nonresiliences associated with $\kappa = 1$ and $\kappa = \infty$ is less than 5%. With $t_l = 30$ years, the nonresilience equals 0.313 when $\kappa = 1$, which is 2.1 times that with infinite resources ($\kappa = \infty$).

For comparison purpose, the time-dependent nonresilience evaluated through Monte Carlo simulation is also presented in Fig. 4. The agreement between the analytical and simulated results demonstrates the accuracy of Eq. (38). Furthermore, using the Matlab R2023a software on a PC with a processor of Intel(R) Core(TM) i7-8700 CPU @ 3.20GHz, the analytical method (Eq. (38)) takes less than 0.5 second to compute Res(50, 2), while the simulation method needs more than one minute (with 100,000 replications of simulation). This comparison demonstrates that the proposed closed form solution for resilience is computationally efficient.

In Fig. 5, the effect of η (i.e., the shape of gradual deterioration) on nonresilience is evaluated with $\psi = 0.1$, assuming linear recovery processes. The nonresilience associated with $\eta = 0.5$ is the largest at the early stages, but becomes the smallest with a longer reference period. The explanation for this observation is two-fold. First, at the early stages with a large probability of $N(t_l) < \kappa$ (this can be deemed as the case of infinite resources), the square-root deterioration shape leads to the smallest performance in the presence of a fixed Δ, followed by those associated with $\eta = 1$ and $\eta = 2$, respectively. For example, examining the PMF of $N(t_l)$ as shown in Fig. 6(a), the probability of $N(20) < 2$ equals 63.2%, while the probability of $N(20) < 4$ is greater than 99.9%. Thus, for both cases in Fig. 5, the nonresilience with $\eta = 0.5$ is the largest for reference periods up to 20 years. Next, for longer reference periods (e.g., $t_l = 40$ years for $\kappa = 2$, or $t_l = 50$ years for $\kappa = 4$), the nonresilience is dominated by the probability of the following (this corresponds to "part 2" of Eq. (28)),

$$\mathbb{P}\left\{\Delta_{r,\kappa} > \Delta_{0,\kappa+1} \middle| N(t_l) \geq \kappa\right\} = \frac{1}{F_{\widetilde{\Delta}_\kappa}(t_l - \kappa\delta)} \cdot \int_0^\infty F_{\widetilde{\Delta}_\kappa}\left(t_l - \kappa\delta - \frac{x}{(1-\alpha)^{1/\eta}}\right) \cdot f_{\Delta_{\kappa+1}}(x)dx \tag{45}$$

Fig. 6(b) presents the probability of $\Delta_{r,\kappa} > \Delta_{0,\kappa+1}$ conditional on $N(t_l) \geq \kappa$ for $\kappa = 2$ (see the lines with a "∘" symbol) and 4 respectively. The case of $\eta = 2$ results in the greatest $\mathbb{P}\left(\Delta_{r,\kappa} > \Delta_{0,\kappa+1} \middle| N(t_l) \geq \kappa\right)$, accounting for the observation from Fig. 5 that the nonresilience associated with $\eta = 2$ becomes the largest with a long reference period.

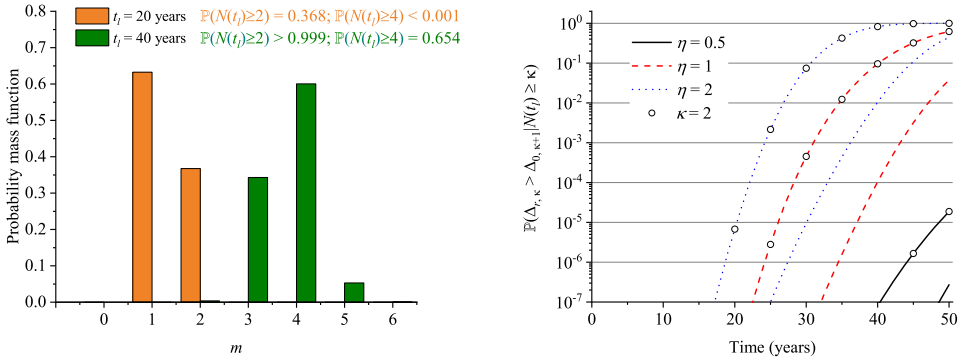

(a) PMF of $N(t_l)$ (b) $\mathbb{P}\left(\Delta_{r,\kappa} > \Delta_{0,\kappa+1} \middle| N(t_l) \geq \kappa\right)$

Fig. 6. Probabilistic behaviors of $N(t_l)$ and $\Delta_{r,\kappa}$.

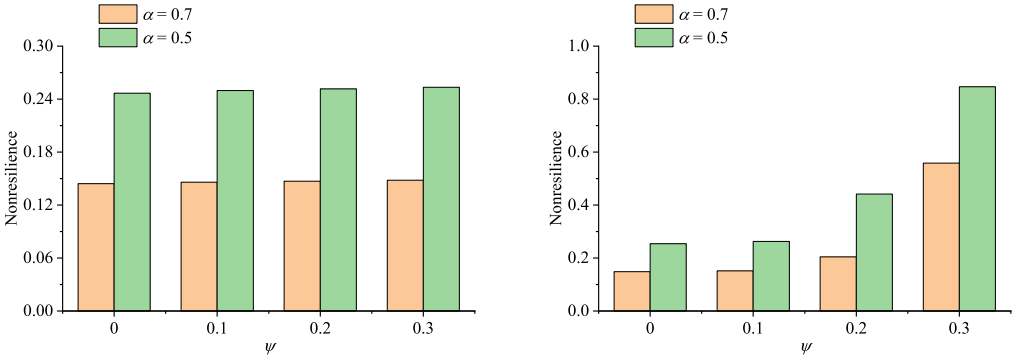

(a) t_l = 20 years (b) t_l = 40 years

Fig. 7. Dependence of nonresilience on α and ψ.

The roles of α and ψ in resilience are shown in Fig. 7, assuming $\eta = \theta = 1$, and $\kappa = 4$. A greater value of α leads to smaller nonresilience, due to the higher performance over the life cycle. Further, a larger ψ indicates that the mean value of the sequence $\{\Delta_1, \Delta_2, \ldots\}$ decreases more rapidly, and thus leads to greater nonresilience. This observation is consistent with those from previous studies that the resilience is weakened in a harsher environment [22,23]. The impact of ψ on resilience is amplified with a longer reference period, due to the increasing number of cycles as shown in Fig. 1.

4.2. Life-cycle resilience of a wind turbine

In this section, a case study on the resilience evaluation of a deteriorating wind turbine is presented, employing the proposed resilience model in Eq. (38). Wind turbines are expected to be safe and resilient to withstand harsh operational environmental during an expected lifetime of 20–25 years [24,25], but have a typical service life between 5 and 13 years [26, Section 1]. One of the most critical components in a wind turbine is the gearbox. Due to the structural changes (e.g., imbalance, damaged bearing races, etc) in the service life, an abnormal vibration response of gearbox will be generated, leading to the deterioration of equipment performance, as illustrated in Fig. 8(a). Gearbox-related failures account for more than 20% the downtime of wind turbines [27, Section 1], and thus will be the focus of this example. Fig. 8(b) shows the time-variant vibration response of a gearbox bearing [28, Table 1], suggesting an accelerated rate of vibration amplitude with time. This motivates the selection of a parabolic model for the performance deterioration process of a wind turbine. The serviceability of gearbox is categorized into different levels according to the vibration response, e.g., level 1 if the vibration amplitude reaches 2.3 mm, and level 5 if exceeding 28 mm, as shown in Fig. 8(b). It takes 9.07 years for the gearbox to reach level 5 in Fig. 8(b), with which the major replacement is conducted. According to [29, Fig. 13], the major replacement of gearbox takes 231 hours, or equivalently 0.079 years (28.88 days) corresponding to 8 work hours per day. A linear recovery process of performance is used herein. In this example, the time that the gearbox takes to reach level 5 is a Gamma variable with a mean value of 9.07 years and a COV of 0.165, with which the service life is within the range of 5–13 years with a probability of 99%. Furthermore, by noting the less lifetime of gearboxes in a changing environment (e.g., increasing intensity of wind loads), the scenarios that the gearbox lifetime degrades by 20%, 10% or 5% compared with that of the replaced one will be examined.

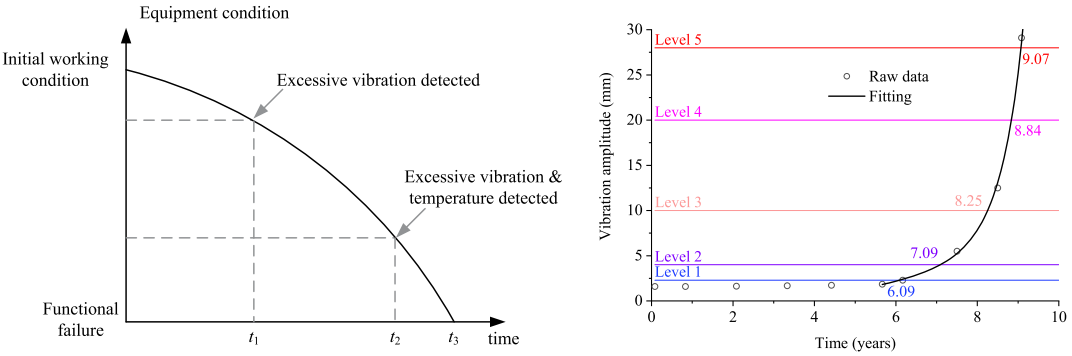

Fig. 8. Time-variant performance of a wind turbine. (a) Deterioration process of performance and condition threshold (after [11]). (b) Deterioration of vibration performance of gearbox bearing, with raw data adopted from [28].

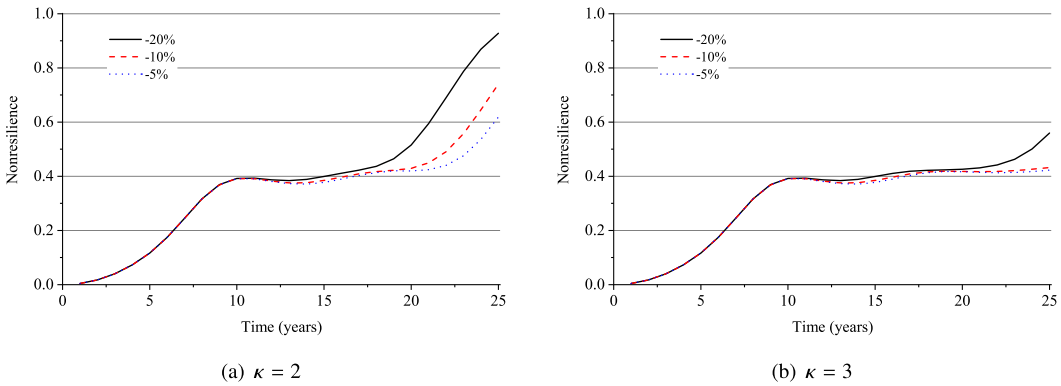

Fig. 9. Time-dependent nonresilience of a wind turbine gearbox.

Fig. 9 presents the time-dependent nonresilience of the wind turbine gearbox for service periods up to 25 years. With a larger value of κ (i.e., greater amount of resources that support the performance recovery), the nonresilience becomes smaller, which is consistent with the observation from Fig. 5. In the presence of a more severe scenario of changing environment, reflected through the more significant degradation of gearbox lifetime, the time-dependent nonresilience is amplified. For example, with $\kappa = 2$, the nonresilience for a reference period of 25 years equals 0.928 if the gearbox lifetime degrades by 20% compared with the replaced one, which becomes 0.619 if the lifetime degrades by 5%. However, the effect of gearbox lifetime degradation on resilience is weakened by a greater value of κ, which implies the importance of resource availability to ensure the turbine resilience against the impacts of climate change.

4.3. Reliability and resilience-based design of a new bridge

In this example, we consider the design of a new reinforced concrete bridge simultaneously guided by the reliability and resilience goals. Assume that the bridge is located in St. Louis (Missouri, USA) and is subjected to the impact of seismic excitation. In the traditional reliability-based design, the aim is to determine the initial resistance of the bridge so that the probability of failure is below a predefined threshold during its service life. According to the ASCE Standard 7 [30, Table 1.3–1], for a structure whose failure is either sudden or leads to widespread progression of damage, the target annual probability of failure, p_{target}, is 3.0×10^{-5} for Risk Category I, corresponding to a target reliability index of 3 based on a 50-year service period (the target failure probability for other risk categories are also available in [30]), which will be used in the following. The seismic hazard for the bridge is given by the "Unified Hazard Tool" provided by the United States Geological Survey (USGS) [31]. Wang and Teh fitted the seismic hazard curve with a unit of g (gravitational acceleration) using an Extreme Type IIdistribution for St. Louis, and determined the shape and scale parameters as 1.617 and 1.98×10^{-3}, respectively (see its CDF in Eq. (A.1)) [32, Fig. 3].

As suggested by Nowak and Szerszen [33, Table 2], the bridge's resistance is a lognormal random variable with a bias factor of 1.14 (thus a mean value of $1.14r_{\text{n}}$, with r_{n} being the nominal resistance) and a coefficient of variation (COV) of 0.13 considering a moment-related limit state function. The requirement on r_{n} is determined based on the target probability failure according to $p(r_{\text{n}}) \leq p_{\text{target}}$, in which $p(r_{\text{n}})$ is the failure probability conditional on r_{n}. This further yields $r_{\text{n}} = 1.2g$. However, the traditional reliability-based design method does not account for the "resilience" of the target structure, thus motivating a new design practice that meets the reliability and resilience goals simultaneously.

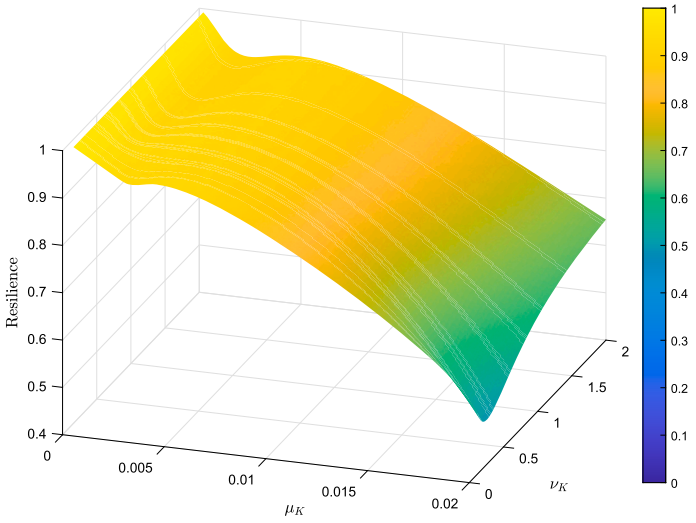

Fig. 10. Time-dependent resilience as a joint function of μ_K and ν_K.

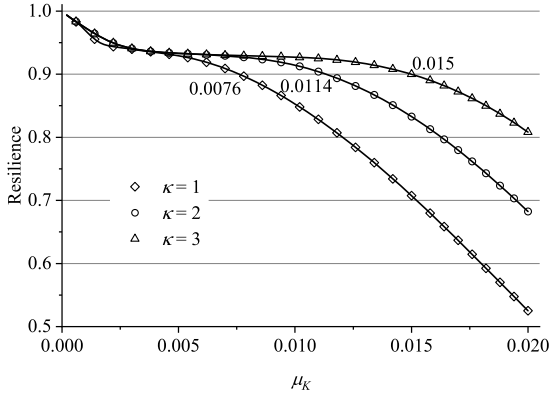

Fig. 11. Time-dependent resilience as a function of μ_K for different values of κ.

Now, we further consider the resilience of the bridge for a service period of 50 years. The resistance degrades with time due to the impact of corrosion, with which we can model the resistance deterioration as a linear process with time [19]. With this regard, let $R(t) = R_0(1 - Kt)$ be the resistance at time t, where R_0 is the initial resistance, and K is the deterioration rate (an inverse Gamma random variable with a mean value of μ_K and a COV of ν_K). Correspondingly, the deterioration of the bridge's performance function is modeled to be in parallel with the resistance deterioration. Once the bridge's resistance degrades by 15% that of the initial state (thus $\alpha = 0.85$), maintenance strategies are conducted immediately to restore the bridge's performance linearly with time based on an "as-good-as-new" strategy (i.e., the resistance is restored via the maintenance strategy to the "brand new" state, see illustration in [34, Fig. 3]). The duration of maintenance is 15 days, as adopted from [35, Table 3].

Recall that Eq. (38) has been derived by considering the gradual deterioration process of performance only. However, in the presence of load event-induced failure mode (e.g., earthquake), the resilience in Eq. (38) holds only if there is no load-induced failure over the life cycle. Thus, Eq. (38) is modified as follows for use in this example,

$$\mathrm{Res}_{\mathrm{load}}(t_l, \kappa) = \mathrm{Rel}_{\mathrm{load}}(t_l) \cdot \underbrace{\mathrm{Res}(t_l, \kappa)}_{\text{Eq. (38)}} \tag{46}$$

where $\mathrm{Res}_{\mathrm{load}}(t_l, \kappa)$ is the resilience considering load-induced failure, and $\mathrm{Rel}_{\mathrm{load}}(t_l)$ refers to the probability that the load effect does not exceed the resistance at any time over $[0, t_l]$ (this is different from the reliability in Eq. (43)). The explicit solution to $\mathrm{Rel}_{\mathrm{load}}(t_l)$ is discussed in Appendix A.

Fig. 10 shows the dependence of nonresilience on both μ_K and ν_K, computed by Eq. (46). A greater value of μ_K or ν_K results in smaller resilience. However, the resilience is more sensitive to the variation of μ_K, which dominates the deterioration rate of resistance. Thus, we can use the term μ_K as a design parameter in the presence of a resilience goal. Fig. 11 presents the dependence of the time-dependent resilience over a service period of 50 years on μ_K with a fixed $\nu_K = 0.5$ and different values of κ (i.e., the resistance can be restored for at most κ times). With a target resilience of 0.9 over 50 years, we can determine the maximum values

of μ_K as 0.0076, 0.0114 and 0.015, respectively, corresponding to $\kappa = 1, 2, 3$. Such information can be used to guide the design of structures to meet the predefined resilience goals, in conjunction with the reliability targets, where the proposed resilience model in this paper plays a vital role, providing an explicit and efficient tool for resilience assessment (the analysis would be time-consuming if using a simulation-based method).

5. Concluding remarks

In this paper, a closed-form method has been developed for the time-dependent resilience assessment of aging structures or systems, taking into account the impact of a changing environment. The proposed resilience model has also incorporated the role of resource availability that supports the recovery of degraded performance. The accuracy and efficiency of the proposed method have been demonstrated via comparison with Monte Carlo simulation. The following conclusions can be made from this paper.

1. The proposed resilience method captures the uncertainty associated with the time-varying performance function within a reference period of interest, and is more efficient compared with Monte Carlo simulation in terms of computational times needed.
2. In the presence of a more severe scenario of change environment, reflected through the more rapid deteriorating rate of performance function (or equivalently, the time it needs to be replaced/repaired), the nonresilience will be amplified (e.g., from 0.254 for a zero deteriorating rate to 0.847 for a deteriorating rate of 0.3 in Fig. 7(b) with a performance threshold of 0.5), implying that the projection of future changes in the number of cycles plays an essential role in resilience assessment.
3. A greater amount of resources will reduce the nonresilience (from 0.313 for at most one time recovery to 0.149 for unlimited resources within a reference period of 30 years), which will thus counter the impact of a changing environment. This demonstrates the importance of recovery-supporting resources to guarantee resilience, requiring the preparedness and readiness of resources from the asset owners/managers.
4. The proposed resilience method can be used to efficiently guide the design of a new structure given a resilience target, in conjunction with the existing reliability-based design method. While the initial resistance of a structure is determined by the target failure probability, the resilience goal raises additional requirement on the life-cycle performance function, and thus the deterioration rate of performance.

Finally, note that the resilience models in this paper (Eqs. (27) and (38)) have been based on a Gamma distributed time duration for the performance function degrading from 1 to a predefined threshold. If this time duration cannot be modeled/approximated by a Gamma distribution, one would need to re-derive the solution for time-dependent resilience, following a similar procedure as in Eqs. (27) and (38). This is a promising topic for future work.

CRediT authorship contribution statement

Cao Wang: Writing – review & editing, Writing – original draft, Visualization, Validation, Supervision, Software, Resources, Project administration, Methodology, Investigation, Funding acquisition, Formal analysis, Data curation, Conceptualization.

Declaration of competing interest

The author declares that he has no known competing financial interests or personal relationships that could have appeared to influence the work reported in this paper.

Data availability

Data will be made available on request.

Acknowledgements

This research described in this paper was supported by the Australian Government through the Australian Research Council's Discovery Early Career Researcher Award (DE240100207). This support is gratefully acknowledged. The views expressed herein are those of the author and are not necessarily those of the Australian Government or Australian Research Council. The author would like to acknowledge the thoughtful suggestions of the Associate Editor and two anonymous reviewers, which substantially improved the present paper.

Appendix A. The time-dependent reliability in Eq. (46)

In this Section, we will derive the time-dependent reliability $\mathrm{Rel}_{\mathrm{load}}(t_l)$ in Eq. (46). This will benefit from the reliability method in Ref. [32].

We use the Extreme Type IIdistribution to model the annual maximum seismic intensity (e.g., the peak ground acceleration), whose CDF is as follows,

$$F_y(x) = \exp\left[-\left(\frac{x}{\epsilon_y}\right)^{-\zeta}\right], \quad x > 0 \tag{A.1}$$

where $\epsilon_y > 0$ and $\zeta > 0$ are the scale and shape parameters, respectively. Further, we let $f_{R_0}(r)$ be the PDF of R_0.

We start from considering the reliability over a subset of $[0, t_l]$, denoted by $[0, t_s]$, over which the resistance degrades to α. Thus we have $K = k = (1-\alpha)/t_s$. We subdivide $[0, t_s]$ into n identical intervals (where $n \to \infty$), denoted by $[t_0 = 0, t_1], [t_1, t_2] \ldots [t_{n-1}, t_n = t_s]$. With this, the maximum seismic intensity within each interval also follows an Extreme Type IIdistribution with a shape parameter of ζ and a scale parameter of $\epsilon_n = \epsilon_y \cdot (t_s/n)^{1/\zeta}$ (its CDF is denoted by $F_n(x)$). Based on the definition of reliability, it follows that,

$$\begin{aligned}
\mathrm{Rel}_{\mathrm{load}}(t_s) &= \mathbb{E}\left\{\prod_{i=1}^{n} F_n\left[R_0 \cdot (1 - kt_i)\right]\right\} \text{ (with respect to } R_0) \\
&= \mathbb{E}\left\{\prod_{i=1}^{n} \exp\left[-\left(\frac{R_0 \cdot (1-kt_i)}{\epsilon_y \cdot (t_s/n)^{1/\zeta}}\right)^{-\zeta}\right]\right\} \\
&= \mathbb{E}\left\{\exp\left\{-\sum_{i=1}^{n} \frac{t_s}{n}\left[\frac{R_0 \cdot (1-kt_i)}{\epsilon_y}\right]^{-\zeta}\right\}\right\} \\
&= \mathbb{E}\left\{\exp\left\{-R_0^{-\zeta}\epsilon_y^{\zeta}\int_0^{t_s}(1-kt)^{-\zeta}dt\right\}\right\} \\
&= \mathbb{E}\left\{\exp\left\{R_0^{-\zeta}\epsilon_y^{\zeta} \cdot \frac{(1-kt_s)^{1-\zeta}-1}{k(1-\zeta)}\right\}\right\} \\
&= \mathbb{E}\left\{\exp\left\{R_0^{-\zeta}\epsilon_y^{\zeta} t_s \cdot \frac{\alpha^{1-\zeta}-1}{(1-\alpha)(1-\zeta)}\right\}\right\}
\end{aligned} \tag{A.2}$$

Now, for the service period of $[0, t_l]$, due to the multiple times of repair measures, the resistance is in a "brand new" state at times $S_0, S_1, S_2 \ldots$ (see Fig. 1). Thus, we denote $t_{s,i} = \Delta_i + \delta$ for $i = 1, 2, \ldots N(t_l)$, and $t_{s,N(t_l)+1} = \Delta_r$. We also model the initial resistance is fully correlated with the restored resistances at times $S_1, S_2 \ldots$. With this, we have,

$$\begin{aligned}
\mathrm{Rel}_{\mathrm{load}}(t_l) &= \prod_{i=1}^{N(t_l)+1} \mathbb{E}\left\{\exp\left\{R_0^{-\zeta}\epsilon_y^{\zeta} t_{s,i} \cdot \frac{\alpha^{1-\zeta}-1}{(1-\alpha)(1-\zeta)}\right\}\right\} \\
&= \mathbb{E}\left\{\exp\left\{R_0^{-\zeta}\epsilon_y^{\zeta} \cdot \frac{\alpha^{1-\zeta}-1}{(1-\alpha)(1-\zeta)} \cdot \sum_{i=1}^{N(t_l)+1} t_{s,i}\right\}\right\} \\
&= \mathbb{E}\left\{\exp\left[R_0^{-\zeta}\epsilon_y^{\zeta} \cdot \frac{\alpha^{1-\zeta}-1}{(1-\alpha)(1-\zeta)} \cdot t_l\right]\right\} \\
&= \int_0^{\infty} \exp\left[r_0^{-\zeta}\epsilon_y^{\zeta} \cdot \frac{\alpha^{1-\zeta}-1}{(1-\alpha)(1-\zeta)} \cdot t_l\right] \cdot f_{R_0}(r_0)
\end{aligned} \tag{A.3}$$

Eq. (A.3) presents a closed form solution for the time-dependent reliability $\mathrm{Rel}_{\mathrm{load}}(t_l)$, which can be used in Eq. (46) for resilience assessment.

References

[1] M.G. Stewart, X. Wang, M.N. Nguyen, Climate change impact and risks of concrete infrastructure deterioration, Eng. Struct. 33 (4) (2011) 1326–1337.
[2] M. Bruneau, S.E. Chang, R.T. Eguchi, et al., A framework to quantitatively assess and enhance the seismic resilience of communities, Earthq. Spectra 19 (4) (2003) 733–752.
[3] C. Wang, B.M. Ayyub, Time-dependent resilience of repairable structures subjected to nonstationary load and deterioration for analysis and design, ASCE-ASME J. Risk Uncertainty Eng. Syst. Part A: Civ. Eng. 8 (3) (2022) 04022021.
[4] D.Y. Yang, D.M. Frangopol, Life-cycle management of deteriorating civil infrastructure considering resilience to lifetime hazards: a general approach based on renewal-reward processes, Reliab. Eng. Syst. Saf. 183 (2019) 197–212.
[5] L. Iannacone, N. Sharma, A. Tabandeh, P. Gardoni, Modeling time-varying reliability and resilience of deteriorating infrastructure, Reliab. Eng. Syst. Saf. 217 (2022) 108074.
[6] K.A.T. Vu, M.G. Stewart, Structural reliability of concrete bridges including improved chloride-induced corrosion models, Struct. Saf. 22 (4) (2000) 313–333.
[7] B.R. Ellingwood, Risk-informed condition assessment of civil infrastructure: state of practice and research issues, Struct. Infrastruct. Eng. 1 (1) (2005) 7–18.
[8] F. Biondini, D.M. Frangopol, Life-cycle performance of deteriorating structural systems under uncertainty, J. Struct. Eng. 142 (9) (2016) F4016001.
[9] L. Capacci, F. Biondini, D.M. Frangopol, Resilience of aging structures and infrastructure systems with emphasis on seismic resilience of bridges and road networks, Resil. Cities Struct. 1 (2) (2022) 23–41.
[10] S.-I. Yang, D.M. Frangopol, L.C. Neves, Optimum maintenance strategy for deteriorating bridge structures based on lifetime functions, Eng. Struct. 28 (2) (2006) 196–206.

[11] B. Le, J. Andrews, Modelling wind turbine degradation and maintenance, Wind Energy 19 (4) (2016) 571–591.
[12] C. Wang, B.M. Ayyub, W.G.P. Kumari, Resilience model for coastal-building foundations with time-variant soil strength due to water intrusion in a changing climate, Rock Soil Mech. 44 (2023) 67–74.
[13] Y. Liu, S. McNeil, Using resilience in risk-based asset management plans, Transp. Res. Rec. 2674 (4) (2020) 178–192.
[14] M. Shadabfar, M. Mahsuli, Y. Zhang, et al., Resilience-based design of infrastructure: review of models, methodologies, and computational tools, ASCE-ASME J. Risk Uncertainty Eng. Syst. Part A: Civ. Eng. 8 (1) (2022) 03121004.
[15] C. Wang, B.M. Ayyub, M. Beer, From reliability-based design to resilience-based design, ASCE-ASME J. Risk Uncertainty Eng. Syst. Part B: Mech. Eng. 9 (3) (2023) 031105.
[16] P. Omidian, N. Khaji, A total life-cycle cost–resilience optimization framework for infrastructures management using different retrofit strategies, Sustain. Resil. Infrastruct. 8 (6) (2023) 675–698.
[17] C. Wang, A generalized index for functionality-sensitive resilience quantification, Resil. Cities Struct. 2 (1) (2023) 68–75.
[18] M. Mead, Generalized inverse gamma distribution and its application in reliability, Commun. Stat., Theory Methods 44 (7) (2015) 1426–1435.
[19] Y. Mori, B.R. Ellingwood, Reliability-based service-life assessment of aging concrete structures, J. Struct. Eng. 119 (5) (1993) 1600–1621.
[20] C. Wang, A stochastic process model for resistance deterioration of aging bridges, Adv. Bridge Eng. 1 (1) (2020) 3.
[21] U. Brandes, Network Analysis: Methodological Foundations, Springer Science & Business Media, 2005.
[22] L.M. Shakou, J.-L. Wybo, G. Reniers, G. Boustras, Developing an innovative framework for enhancing the resilience of critical infrastructure to climate change, Saf. Sci. 118 (2019) 364–378.
[23] C. Wang, B.M. Ayyub, A. Ahmed, Time-dependent reliability and resilience of aging structures exposed to multiple hazards in a changing environment, Resilient Cities Struct. 1 (3) (2022) 40–51.
[24] V.L. Jantara Jr, M. Papaelias, Wind turbine gearboxes: failures, surface treatments and condition monitoring, in: Non-Destructive Testing and Condition Monitoring Techniques for Renewable Energy Industrial Assets, Elsevier, 2020, pp. 69–90.
[25] D. Wilkie, C. Galasso, Impact of climate-change scenarios on offshore wind turbine structural performance, Renew. Sustain. Energy Rev. 134 (2020) 110323.
[26] E.J. Alvarez, A.P. Ribaric, An improved-accuracy method for fatigue load analysis of wind turbine gearbox based on scada, Renew. Energy 115 (2018) 391–399.
[27] G. Mandic, A. Nasiri, E. Muljadi, F. Oyague, Active torque control for gearbox load reduction in a variable-speed wind turbine, IEEE Trans. Ind. Appl. 48 (6) (2012) 2424–2432.
[28] J. Li, X. Zhang, X. Zhou, L. Lu, Reliability assessment of wind turbine bearing based on the degradation-hidden-markov model, Renew. Energy 132 (2019) 1076–1087.
[29] J. Carroll, A. McDonald, D. McMillan, Failure rate, repair time and unscheduled O&M cost analysis of offshore wind turbines, Wind Energy 19 (6) (2016) 1107–1119.
[30] ASCE, Minimum Design Loads for Buildings and Other Structures, ASCE 7-22, American Society of Civil Engineers, 2022.
[31] USGS, Unified hazard tool, https://earthquake.usgs.gov/hazards/interactive/index.php. (Accessed 10 September 2024), 2024, online resource.
[32] C. Wang, L.H. Teh, Time-dependent seismic reliability of aging structures, ASCE-ASME J. Risk Uncertainty Eng. Syst. Part A: Civ. Eng. 8 (2) (2022) 04022010.
[33] A.S. Nowak, M.M. Szerszen, Bridge load and resistance models, Eng. Struct. 20 (11) (1998) 985–990.
[34] B.M. Ayyub, Systems resilience for multihazard environments: definition, metrics, and valuation for decision making, Risk Anal. 34 (2) (2014) 340–355.
[35] X. Mao, X. Jiang, C. Yuan, J. Zhou, Modeling the optimal maintenance scheduling strategy for bridge networks, Appl. Sci. 10 (2) (2020) 498.